



University of Pennsylvania
ScholarlyCommons

Departmental Papers (ESE)

Department of Electrical & Systems Engineering

1-27-2012

Boosting Optical Nonlinearities in ϵ -Near-Zero Plasmonic Channels

Christos Argyropoulos
University of Texas at Austin

Pai-Yen Chen
University of Texas at Austin

Giuseppe D'Aguanno
AEgis Technologies Group

Nader Engheta
University of Pennsylvania, engheta@ee.upenn.edu

Andrea Alù
University of Texas at Austin

Follow this and additional works at: http://repository.upenn.edu/ese_papers

 Part of the [Engineering Commons](#), and the [Physics Commons](#)

Recommended Citation

Christos Argyropoulos, Pai-Yen Chen, Giuseppe D'Aguanno, Nader Engheta, and Andrea Alù, "Boosting Optical Nonlinearities in ϵ -Near-Zero Plasmonic Channels", . January 2012.

Argyropoulos, C., Chen, P., D'Aguanno, G., Engheta, N., & Alù, A. (2012). Boosting optical nonlinearities in ϵ -near-zero plasmonic channels. *Physical Review B*, 85(4), 045129. doi: [10.1103/PhysRevB.85.045129](https://doi.org/10.1103/PhysRevB.85.045129)

©2012 American Physical Society

This paper is posted at ScholarlyCommons. http://repository.upenn.edu/ese_papers/608

For more information, please contact repository@pobox.upenn.edu.

Boosting Optical Nonlinearities in ϵ -Near-Zero Plasmonic Channels

Abstract

The anomalous transmission properties of zero-permittivity ultranarrow channels are used to boost Kerr nonlinearities and achieve switching and bistable response for moderate optical intensities. Strong field enhancement, uniform all along the channel, is a typical feature of ϵ -near-zero supercoupling and is shown to be particularly suited to enhance nonlinear effects. This is obtained by designing narrow apertures at cutoff in a plasmonic screen. We show that this nonlinear mechanism can significantly outperform nonlinearities in traditional Fabry-Pérot resonant gratings.

Disciplines

Engineering | Physics

Comments

Argyropoulos, C., Chen, P., D'Aguanno, G., Engheta, N., & Alù, A. (2012). Boosting optical nonlinearities in ϵ -near-zero plasmonic channels. *Physical Review B*, 85(4), 045129. doi: [10.1103/PhysRevB.85.045129](https://doi.org/10.1103/PhysRevB.85.045129)

©2012 American Physical Society

Boosting optical nonlinearities in ϵ -near-zero plasmonic channels

Christos Argyropoulos,¹ Pai-Yen Chen,¹ Giuseppe D'Aguanno,² Nader Engheta,³ and Andrea Alù^{1,*}

¹*Department of Electrical & Computer Engineering, University of Texas at Austin, Austin, Texas, USA*

²*AEgis Technologies Group, Nanogenesis Division, Huntsville, Alabama 35806, USA*

³*Department of Electrical and Systems Engineering, University of Pennsylvania, Philadelphia, Pennsylvania, USA*

(Received 4 January 2012; published 27 January 2012)

The anomalous transmission properties of zero-permittivity ultranarrow channels are used to boost Kerr nonlinearities and achieve switching and bistable response for moderate optical intensities. Strong field enhancement, uniform all along the channel, is a typical feature of ϵ -near-zero supercoupling and is shown to be particularly suited to enhance nonlinear effects. This is obtained by designing narrow apertures at cutoff in a plasmonic screen. We show that this nonlinear mechanism can significantly outperform nonlinearities in traditional Fabry-Pérot resonant gratings.

DOI: [10.1103/PhysRevB.85.045129](https://doi.org/10.1103/PhysRevB.85.045129)

PACS number(s): 41.20.Jb, 42.65.Wi, 71.45.Gm, 78.67.Pt

I. INTRODUCTION

Considerable interest has been recently devoted to artificial media with anomalous values of effective permittivity and permeability. Extreme constitutive parameters,¹ very low²⁻⁵ or very high^{7,8} compared to those available in nature, are especially attractive for a variety of applications, including subwavelength imaging,⁹ radiation patterning,^{2,5} and optical nanocircuits.^{10,11} Zero-permittivity (ENZ) metamaterials have raised special interest due to their anomalous *quasistatic* response that provides “infinite” phase velocity of propagation, and to their arguably simple realization.¹² One of the most dramatic effects of ENZ materials is obtained when they are used to fill an ultranarrow channel: perfectly matched transmission has been theoretically predicted at the discontinuity between a much larger waveguide and such ENZ channels,^{3,4} and these concepts have been experimentally verified at microwaves.^{6,13} The associated *large* field enhancement, *uniform* all along the channel due to the ENZ quasistatic response, is peculiarly independent of its length and shape and it has been proposed for exciting concepts in light concentration and harvesting,¹⁴ sensors,¹⁵ and boosting molecular emission.¹⁶

These same peculiar transmission properties, with uniformly large electric field enhancement, are particularly attractive when distributed nonlinearities are present all along the channel. Optical nonlinear effects are naturally weak and very large intensities are usually required to achieve nonlinear operations, such as switching and bistabilities. In addition, phase matching is an issue when exciting electrically large nonlinear samples to achieve stronger responses. Resonances may be used to locally enhance nonlinear effects,¹⁷ but they are usually limited in their spatial extent. We propose here an interesting concept to exploit the uniform and constant-phase field enhancement along ENZ channels to boost optical nonlinearities. In this context, we have recently considered a microwave experiment to realize tunable *supercoupling* transmission using a single nonlinear varactor placed inside the ENZ channel.¹⁸ In addition, nonlinear ENZ operation has been recently explored in a theoretical scenario in which optical nonlinearities are assumed in an ideal plasmonic slab with near-zero permittivity (without field enhancement).^{19,20} Here we translate the ENZ concepts, limited in previous papers to closed waveguides,¹⁴⁻¹⁶ to a three-dimensional metamaterial

slab operating in free space, suggesting a route to realize ENZ metamaterials with enhanced nonlinear effects. Our geometry is tailored to support and drastically boost nonlinear effects, outperforming conventional resonant mechanisms for nonlinear operation. When loaded with Kerr nonlinearities, we show a metamaterial slab with bistable and self-tunable response achieved with relatively low threshold intensities, significantly lower than similar effects based on Fabry-Pérot (FP) resonances. This may lead to strong bistability and to the realization of self-tunable slow-light devices, low-intensity optical memories, switches, and tunable sensors.

II. GEOMETRY OF THE PROBLEM

Consider the plasmonic grating in Fig. 1, composed of narrow periodic rectangular slits of width w , height $t \ll w$, length l , and periods $a, b \gg t$, carved in a silver screen with relative Drude permittivity dispersion $\epsilon_{Ag} = \epsilon_\infty - f_p^2/[f(f + i\gamma)]$, $f_p = 2175$ THz, $\gamma = 4.35$ THz, and $\epsilon_\infty = 5$.²¹ The slits are loaded with a standard nonlinear Kerr material, with relative permittivity $\epsilon_{ch} = \epsilon_L + \chi^{(3)}|E_{ch}|^2$, $\epsilon_L = 2.2$, $\chi^{(3)} = 4.4 \times 10^{-20}$ m²/V², typical values for nonlinear optical materials,²² and $|E_{ch}|$ is the magnitude of the local electric field in the channel. Since the slits occupy a small area of the grating surface, impinging incident waves are mostly reflected at the first interface, and extraordinary optical transmission (EOT) resonances typically occur for Fabry-Pérot or grating resonances.^{23,24} By filling similar slits or gratings with nonlinear materials, optical bistability around the EOT resonances has been theoretically predicted in.²⁵ Here, we aim at operating in an alternative resonant transmission regime, based on ENZ supercoupling transmission within each rectangular slit, for which uniform field enhancement all along the channel may significantly enhance the nonlinear operation. Similar to the supercoupling effect in closed waveguides,¹⁴ we tailor each slit width to operate *exactly* at the cutoff of its dominant quasi-TE₁₀ mode, i.e., at the frequency for which its guided wave number β has a near-zero real part and minimum imaginary part, assuming an $e^{i\beta z}$ propagation factor inside each slit. This ensures that (a) the guided wavelength in each slit is effectively infinite and (b) the corresponding characteristic impedance is also very large, compensating the impedance mismatch at

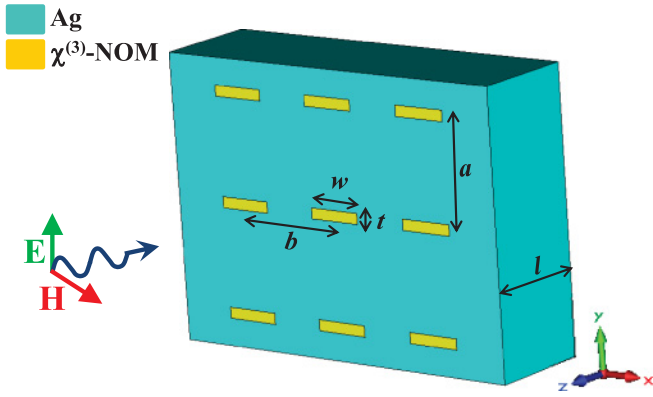


FIG. 1. (Color online) Nonlinear ENZ metamaterial slab obtained by carving narrow rectangular apertures loaded with nonlinear optical materials in a silver screen. The device is illuminated at normal incidence by a plane wave.

the transition between each narrow slit and free space. These properties result in an anomalous matching phenomenon that produces total transmission, large field enhancement in the slits and uniform phase, a combination of properties extremely well suited to boosting optical nonlinearities. Note that similar findings were demonstrated in the past for a thin slab patterned with a single rectangular hole^{26,27} and for complicated slit designs patterned again on a thin slab at microwave frequencies,^{28,29} where in both cases nonlinearities were not included.

III. THEORETICAL ANALYSIS

The cutoff condition for a rectangular plasmonic waveguide may be obtained for $\text{Re}[\epsilon_{\text{Ag}}] \ll -1$ by requiring that the guided wavelength $2\pi/\beta_{\text{pp}}$ (where β_{pp} is the guided wave number) in the associated parallel-plate plasmonic waveguide with the same height t as the slit, but infinite width,³⁰ is twice the effective slit width

$$\frac{\beta_{\text{pp}}}{k_0\sqrt{\epsilon_{\text{ch}}}} = \frac{\pi}{\beta_{\text{pp}}w + 2\sqrt{\epsilon_{\text{ch}}}/\sqrt{\text{Re}[-\epsilon_{\text{Ag}}]}}, \quad (1)$$

where k_0 is the free-space wave number. Equation (1) takes into account the modal dispersion in a plasmonic channel and tends to the classic cutoff condition $w = \pi/(k_0\sqrt{\epsilon_{\text{ch}}})$ when $\beta_{\text{pp}} = k_0\sqrt{\epsilon_{\text{ch}}}$, for $\epsilon_{\text{Ag}} \rightarrow -\infty$ (perfectly conducting slits). In general, when Eq. (1) is satisfied, each plasmonic slit is at cutoff and its dominant quasi-TE₁₀ mode “feels” an effective near-zero permittivity.

Applying a transmission-line model to describe the wave interaction with the grating, inspired by the approach used in³¹ for a different scattering problem, we may describe each aperture as a two-dimensional slit with effective permittivity

$$\epsilon_{\text{eff}} = \frac{\beta_{\text{pp}}^2}{k_0^2} - \frac{\pi^2\epsilon_{\text{ch}}}{(\beta_{\text{pp}}w + 2\sqrt{\epsilon_{\text{ch}}}/\sqrt{\text{Re}[-\epsilon_{\text{Ag}}]})^2}. \quad (2)$$

The effect of nonlinearity is implicit in Eq. (2), as both β_{pp} and ϵ_{ch} depend on $\chi^{(3)}|E_{\text{ch}}|^2$. In particular, in the limit $\epsilon_{\text{Ag}} \rightarrow -\infty$, we may explicitly write

$$\epsilon_{\text{eff}} = \epsilon_L - \frac{\pi^2}{k_0^2w^2} + \frac{b^2a^2}{w^2t^2}\chi^{(3)}|E_{\text{in}}|^2, \quad (3)$$

where E_{in} is the electric field impinging on the screen, where we have used power conservation at the discontinuities in the E and H planes of the slit to evaluate the enhancement factor $E_{\text{ch}} = (ba)E_{\text{in}}/(tw)$. Equation (3) ensures that the slits act as if filled with an effective ENZ metamaterial with drastically enhanced Kerr coefficient $\frac{b^2a^2}{w^2t^2}\chi^{(3)}$. Due to the infinite phase velocity near the ENZ operation, we can safely neglect the magnitude and phase variation of E_{ch} along z , and assume a homogeneous filling material with ENZ and enhanced nonlinear properties. These concepts may be used to verify in a practical scenario the anomalous bistability features of ideal nonlinear ENZ slabs predicted in Ref. 20. Here, we propose to use them in an even more intriguing scenario, in which the nonlinear effects are drastically boosted by the large geometrical mismatch between free space and the narrow slits, leading to enhanced bistability features for optical memories and switches, as we discuss in the following.

A. Linear operation

We consider first the linear operation of the grating, for $\chi^{(3)}|E_{\text{ch}}|^2 \simeq 0$. We choose the design parameters $w = 200$ nm and $t = 40$ nm to achieve the cutoff condition (1) and linear ENZ operation around the free-space wavelength $\lambda_0 = 1 \mu\text{m}$. We have indeed verified that the grating supports a transmission peak around this frequency, independent of the choice of l or of the periods a, b . For longer wavelengths, the slits operate below cutoff and the impinging waves are almost totally reflected, whereas for shorter wavelengths the usual FP transmission peaks are obtained, under the condition $\beta = N\pi/l$, with N being an integer, as a function of the channel length. Quite distinctly, at the cutoff condition (1) the EOT is obtained based on a matching mechanism at the entrance and exit face of the grating, which has nothing to do with cavity or grating resonances within the channel length or periods, consistent with the concept introduced in Ref. 4 for closed waveguides, but extended here to a three-dimensional metamaterial slab in free space. As expected, the grating period does not affect the ENZ operation, but it affects the field enhancement factor, which is proportional to the ratio $(ab)/(tw)$ in Eq. (3), and its bandwidth of operation. We choose in the following $l = 500$, $a = 400$, and $b = 400$ nm, obtaining for the linear operation, the transmission curves in Fig. 2 [red (gray) lines, same curve in each panel]. As expected, an ENZ transmission peak is obtained at $\lambda_0 = 1017$ nm, and a second peak is obtained at $\lambda_0 = 932$ nm, at the first FP resonance of the slits. The peak transmission is slightly lower for the ENZ resonance, despite the plasmonic properties of silver being more absorptive at shorter wavelengths. This is because the field distribution along the channel is uniform at the ENZ operation, making the wall material (Ag) absorption more effective. In an even stronger way, we expect the nonlinear properties of the Kerr material to be boosted by the anomalous ENZ transmission features. We show in Fig. 3 the field enhancement distribution inside each slit at these two distinct resonances, as computed with full-wave simulations in the linear regime,³² normalized to the impinging signal. The three-dimensional normalized distribution inside the slits is also shown in the insets. Despite the level of transmission being similar at the two resonances, the field distribution is

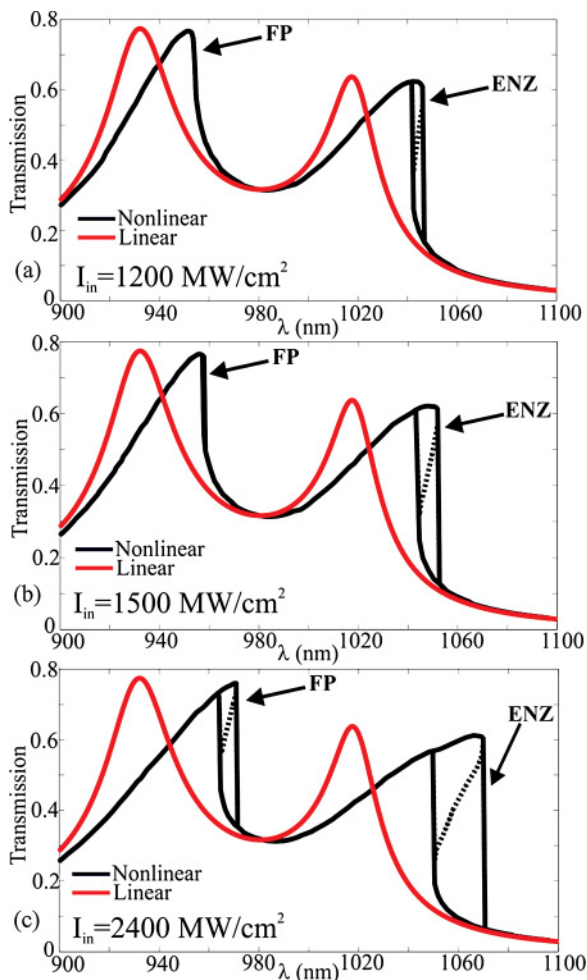


FIG. 2. (Color online) Transmission coefficient vs wavelength for linear and nonlinear operation at three different input intensities: (a) $I_{in} = 1200 \text{ MW/cm}^2$, (b) $I_{in} = 1500 \text{ MW/cm}^2$, (c) $I_{in} = 2400 \text{ MW/cm}^2$. The unstable branches of the bistable curves are shown with dashed lines.

drastically different: uniform and strong field confinement is obtained at the ENZ frequency all over the channel length, as predicted, whereas a typical standing wave distribution is obtained at the FP resonance, with a sharp minimum at the channel center. It is evident that this uniform and phase-constant enhancement is particularly suited to boosting nonlinear and bistable responses once the material nonlinearity in the channel is considered. It is also noted that the average field enhancement is consistent with the approximate value $ab/(tw) \simeq 20$ in Eq. (3), somewhat smaller in the ENZ operation due to the moderately larger absorption.

B. Nonlinear operation

Now we consider the presence of the Kerr effect in the channel. In Fig. 4, we show the variation of nonlinear permittivity versus the impinging intensity at two typical wavelengths of interest, slightly above the two resonant wavelengths for linear operation, in order to obtain bistable response. For a fair comparison, we have selected the two wavelengths to be 2.8% longer than the corresponding ENZ

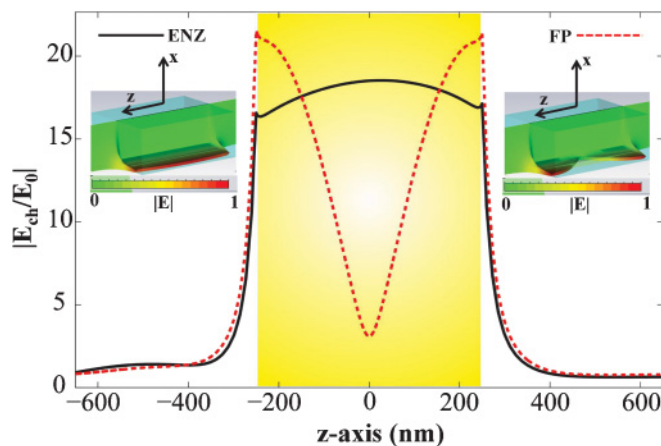


FIG. 3. (Color online) Electric field enhancement distribution along the channel operating at the ENZ operation and at the first FP resonance. The channel is shown with a light yellow (gray) shaded region. The 3D normalized field distributions are shown in the insets.

and FP resonant wavelengths for linear operation considered in Fig. 3. Bistable permittivity dispersion is observed at both wavelengths, but, as predicted, the ENZ resonance supports much stronger hysteresis compared with a usual FP resonance for the same level of nonlinearity and a lower triggering intensity, directly related to the uniformity of the field enhancement in the ENZ operation. It is particularly encouraging to apply these concepts to bistable and self-tunable plasmonic devices.

In this regard, we have considered in Fig. 2 the nonlinear transmission versus wavelength for three different input intensities: (a) $I_{in} = 1200 \text{ MW/cm}^2$, (b) $I_{in} = 1500 \text{ MW/cm}^2$, and (c) $I_{in} = 2400 \text{ MW/cm}^2$. In each panel we also show the linear operation [very low intensity, red (gray) line] to compare the nonlinearity effect. Despite a lower level of transmission peak, the ENZ performance has consistently larger hysteresis and lower triggering intensity value for bistability operation compared to those at the FP resonance. In particular, in Fig. 2(a) the optical intensity is too low ($I_{in} = 1200 \text{ MW/cm}^2$) for the FP resonance to show any bistable effect, whereas the ENZ

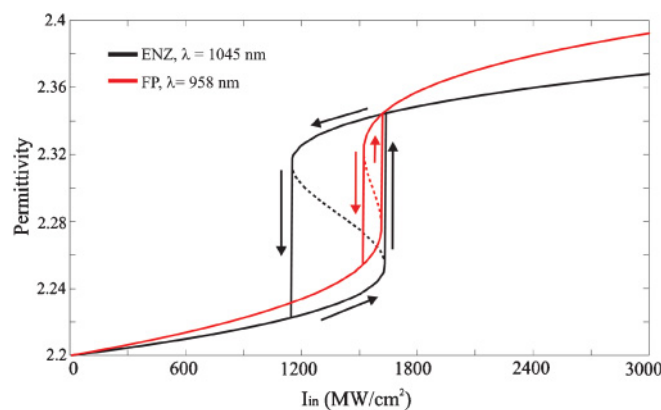


FIG. 4. (Color online) Variation of relative nonlinear permittivity with the impinging light intensity for ENZ and FP operation. The unstable branches are shown with dashed lines.

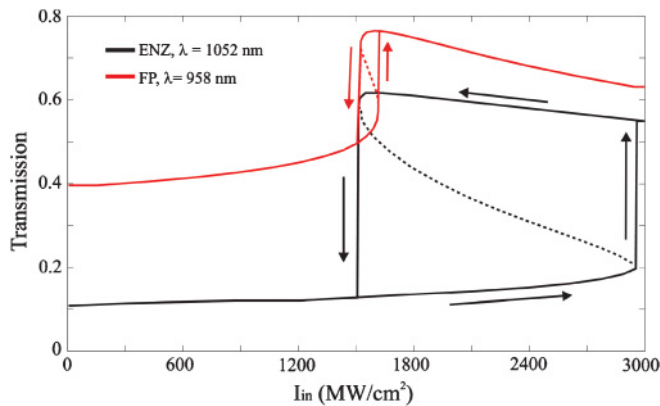


FIG. 5. (Color online) Field transmission as a function of the input intensity for ENZ and FP transmission. The unstable branches are also shown with dashed lines.

channel already shows a clear bistable operation due to the stronger and uniform average fields in the channel. At a triggering intensity $I_{in} = 1500 \text{ MW/cm}^2$ [Fig. 2(b)], bistable effects start to appear in the FP operation, whereas the ENZ channel offers much broader hysteresis. Similar differences are seen also in Fig. 2(c), for a higher input intensity $I_{in} = 2400 \text{ MW/cm}^2$. By comparing Figs. 2(a) and 2(c), it is evident that the ENZ operation may achieve a similar bistability response with half the required intensity, a significant achievement to boost optical nonlinearities. We conclude that the ENZ channel may provide memory and switching effects at lower intensities than typical localized resonant effects, due to its uniform field distribution.

Similarly, Fig. 5 considers the all-optical switching properties of the grating and operating, respectively, at the ENZ and FP resonance. In particular, we show the variation of transmission versus impinging intensity for two specific wavelengths, chosen approximately at the center of the optical bistability regions of Fig. 2(c). We also show the unstable branches as dashed lines. The hysteresis loop of the ENZ channel is much broader, not only in terms of optical intensities, but also in terms of maximum and minimum transmission values, compared with FP transmission. This emphasizes that the ENZ boosting of optical nonlinearities may be used for efficient, ultrathin all-optical switches, as well as for memories. For instance, based on the results of Fig. 5, it is obvious that the transmission through the ENZ grating [black (dark gray) line in Fig. 5] remains almost constant around 0.15 (lower branch of the hysteresis curve) with increasing intensity. This can be considered the OFF operation, when an appropriate transmission threshold is defined. When the input intensity reaches higher values than $I_{in} = 3000 \text{ MW/cm}^2$, the transmission performance switches to the upper branch of the hysteresis curve, around 0.55. Then, when the optical intensity starts to decrease, the transmission takes constant high average values around 0.6. This may be considered the ON mode of the proposed all-optical switch. Again, when the input intensity drops below $I_{in} = 1500 \text{ MW/cm}^2$, the device goes back to OFF operation and the plasmonic switch is closed.

We envision the integration of this metamaterial design with plasmonic devices to realize all-optical integrated systems. The ultralow profile of the grating and its conformability may be integrated using lithographic techniques within optical source designs and in more complex photonic systems. Nonlinear materials are not required to be included only inside the slits, more practically they may also cover the screen and be used as a substrate without affecting the predicted operation of the device, since the field is enhanced only inside the slits. Note that the proposed metamaterial slab can be built using advanced nanofabrication tools, such as nanoskiving,³³ a particularly suitable method to produce arrays of nanostructures. Finally, it is important to stress that the thickness of the plasmonic slab can be chosen smaller than the proposed $l = 500 \text{ nm}$ without affecting the nature of the ENZ resonance and its position at the frequency spectrum.¹⁴ In this case, only the FP resonance will move to lower wavelengths, and both resonances (ENZ and FP) will have increased bandwidth and transmission due to the decreased total absorption of the plasmonic waveguide. As a result, the concept of boosted nonlinearity at the ENZ resonance will be still dominant, stressing more the flexibility and efficiency of our proposed design.

IV. CONCLUSIONS

To conclude, we have shown here an interesting metamaterial concept based on plasmonic gratings loaded with nonlinear optical materials to realize an effective ENZ metamaterial in the visible range with large nonlinear properties. We have shown that strong and uniform field enhancement may be achieved inside the nonlinear ENZ slits, which can efficiently boost nonlinear effects compared with conventional resonances.²⁵ Our ENZ mechanism ensures large hysteresis responses, achievable with relatively low impinging intensities. This property may pave the way to future nonlinear plasmonic devices integrated in all-optical systems, such as self-tunable optical sensing structures, switches, optical memories, and advanced plasmonic nanocircuits. Similar concepts may also be applied to harmonic generators and parametric amplifiers, for which the uniform phase within the channel may be particularly interesting. We stress that the specific plasmonic design proposed in this article is not necessarily the optimal geometry for exploiting the ENZ properties of narrow plasmonic channels at cutoff to enhance nonlinear operation, but it is chosen to provide direct comparison between ENZ and FP or EOT operation and to highlight an alternative physical mechanism to boost optical nonlinearities, based on realistic ENZ metamaterial effects. In this context, it is relevant to mention that the efficiency of nonlinear operation for bistability and switching operation is often associated with the Q factor of the corresponding resonances, and it is commonly believed that lower triggering intensities are associated with higher resonance Q factors.^{34,35} In the example considered here, however, ENZ and FP resonances have comparable bandwidths, and the ENZ operation is even more largely affected by absorption compared to the FP resonance, lowering its overall Q factor. Our results show that another relevant factor plays a role in boosting the nonlinear properties of optical materials, provided by the uniform field enhancement typical of ENZ tunneling effects. To summarize, we have also

demonstrated that low trigger intensities combined with low Q -factor ENZ resonances can achieve broad hysteresis effects, a concept of great potential practical and theoretical interest to the recently introduced field of nonlinear plasmonics. Improved and optimized designs may provide even stronger robustness to losses and larger transmission, as will be explored in future works.

ACKNOWLEDGMENTS

This work has been supported by the ARO STTR project “Dynamically Tunable Metamaterials,” the AFOSR YIP Grant No. FA9550-11-1-0009, the ONR MURI Grant No. N00014-10-1-0942, and the DARPA SBIR project “Non-linear Plasmonic Devices.”

*alu@mail.utexas.edu

- ¹A. Sihvola, S. Tretyakov, and A. de Baas, *J. Commun. Technol. Electron.* **52**, 986 (2007).
- ²A. Alù, M. G. Silveirinha, A. Salandrino, and N. Engheta, *Phys. Rev. B* **75**, 155410 (2007).
- ³M. Silveirinha and N. Engheta, *Phys. Rev. Lett.* **97**, 157403 (2006).
- ⁴A. Alù, M. G. Silveirinha, and N. Engheta, *Phys. Rev. E* **78**, 016604 (2008).
- ⁵R. W. Ziolkowski, *Phys. Rev. E* **70**, 046608 (2004).
- ⁶R. Liu, Q. Cheng, T. Hand, J. J. Mock, T. J. Cui, S. A. Cummer, and D. R. Smith, *Phys. Rev. Lett.* **100**, 023903 (2008).
- ⁷P. B. Catrysse, G. Veronis, H. Shin, J. T. Shen, and S. Fan, *Appl. Phys. Lett.* **88**, 31101 (2006).
- ⁸M. Choi, S. H. Lee, Y. Kim, S. B. Kang, J. Shin, M. H. Kwak, K.-Y. Kang, Y.-H. Lee, N. Park, and B. Min, *Nature* **470**, 369 (2011).
- ⁹M. G. Silveirinha, C. R. Medeiros, C. A. Fernandes, and J. R. Costa, *New J. Phys.* **13**, 053004 (2011).
- ¹⁰M. G. Silveirinha, A. Alù, J. Li, and N. Engheta, *J. Appl. Phys.* **103**, 064305 (2008).
- ¹¹A. Alù and N. Engheta, *Phys. Rev. Lett.* **103**, 143902 (2009).
- ¹²W. Rotman, *IRE Trans. Antennas Propag.* **10**, 82 (1962).
- ¹³B. Edwards, A. Alù, M. E. Young, M. Silveirinha, and N. Engheta, *Phys. Rev. Lett.* **100**, 033903 (2008).
- ¹⁴A. Alù and N. Engheta, *Phys. Rev. B* **78**, 035440 (2008).
- ¹⁵A. Alù and N. Engheta, *Phys. Rev. B* **78**, 045102 (2008).
- ¹⁶A. Alù and N. Engheta, *Phys. Rev. Lett.* **103**, 043902 (2009).
- ¹⁷P. Y. Chen and A. Alù, *Phys. Rev. B* **82**, 235405 (2010).
- ¹⁸D. A. Powell, A. Alù, B. Edwards, A. Vakil, Y. S. Kivshar, and N. Engheta, *Phys. Rev. B* **79**, 245135 (2009).
- ¹⁹A. Ciattoni, C. Rizza, and E. Palange, *Phys. Rev. A* **83**, 043813 (2011).
- ²⁰A. Ciattoni, C. Rizza, and E. Palange, *Opt. Lett.* **35**, 2130 (2010).
- ²¹P. B. Johnson and R. W. Christy, *Phys. Rev. B* **6**, 4370 (1972).
- ²²R. W. Boyd, *Nonlinear Optics* (Academic, London, 1992).
- ²³T. W. Ebbesen, H. J. Lezec, H. F. Ghaemi, T. Thio, and P. A. Wolff, *Nature* **391**, 667 (1998).
- ²⁴F. J. García de Abajo, *Rev. Mod. Phys.* **79**, 1267 (2007).
- ²⁵J. A. Porto, L. Martín-Moreno, and F. J. García-Vidal, *Phys. Rev. B* **70**, 081402(R) (2004).
- ²⁶F. J. García-Vidal, E. Moreno, J. A. Porto, and L. Martín-Moreno, *Phys. Rev. Lett.* **95**, 103901 (2005).
- ²⁷F. J. García-Vidal, L. Martín Moreno, E. Moreno, L. K. S. Kumar, and R. Gordon, *Phys. Rev. B* **74**, 153411 (2006).
- ²⁸J. R. Suckling, J. R. Sambles, and C. R. Lawrence, *Phys. Rev. Lett.* **95**, 187407 (2005).
- ²⁹R. J. Kelly, M. J. Lockyear, J. R. Suckling, J. R. Sambles, and C. R. Lawrence, *Appl. Phys. Lett.* **90**, 223506 (2007).
- ³⁰A. Alù and N. Engheta, *J. Opt. Soc. Am. B* **23**, 571 (2006).
- ³¹A. Alù, G. D’Aguanno, N. Mattiucci, and M. J. Bloemer, *Phys. Rev. Lett.* **106**, 123902 (2011).
- ³²CST Design Studio 2011, [www.cst.com].
- ³³Q. Xu, R. M. Rioux, M. D. Dickey, and G. M. Whitesides, *Acc. Chem. Res.* **41**, 1566 (2008).
- ³⁴G. D’Aguanno, D. de Ceglia, N. Mattiucci, and M. J. Bloemer, *Opt. Lett.* **36**, 1984 (2011).
- ³⁵M. Ren, B. Jia, J.-Y. Ou, E. Plum, J. Zhang, K. F. MacDonald, A. E. Nikolaenko, J. Xu, M. Gu, and N. I. Zheludev, *Adv. Mater.* **23**, 5540 (2011).